

Polar Optical Phonons in AlN/GaN superlattice structures.

J. B. Herzog

Department of Electrical Engineering, University of Notre Dame, Notre Dame, Indiana 46556
Physics of Electron Transport in Semiconductor Devices

(Dated: December 12, 2006)

Infrared reflection spectra of bulk semiconductors and superlattices can be predicted mathematically with optical phonon frequencies as some of the input variables. This method will be used to determine the polar longitudinal and transverse optical phonons modes and their corresponding energies that are present in AlN/GaN superlattices. Theoretical results will be compared to reflection experiments taken at a 75° incidence angle. Different AlN/GaN superlattice combinations will be studied to see if any pattern of phonon energies may arise. This outcome may prove useful in engineering phonons at specific frequencies. Furthermore, new phonons exist that are not at the energy levels present in bulk AlN and GaN. Phonon dispersion curve “folding” might prove useful to predict these new phonons. It will be determined whether this “folding” is a useful explanation for these new phonons, and if not, a new hypothesis will be made.

I. INTRODUCTION

Phonons, which are atomic vibrational waves, greatly affect electron mobility due to scattering. These waves displace atoms in semiconductor crystals which in turn alter the electronic potential and cause electron scattering. In compound semiconductors, like AlN and GaN, the bond is ionic. A phonon in this case alters the dipole between the atoms and creates an electric field. The electric field, due to these polar optical phonon, causes very strong scattering and is typically the dominating scattering mechanism in compound semiconductors[1]. The effects of phonons are not always negative as in the instance of impeding electron mobility. Phonons can be useful in dissipating heat out of semiconductors.

GaN and AlN compounds have been proven useful in wide bandgap microelectronics and optoelectronics[2]. Study of phonon properties in Bulk GaN and AlN has been extensive[3]. Studies have also been done on some superlattices, however, phonon properties of AlN/GaN superlattices are not well known.

With the help of infrared spectroscopy experiential results, characteristics of optical phonon in AlN/GaN superlattices can be understood more. This work has identified some new phonons that are present in these superlattices, yet not present in bulk AlN and GaN. This study will determine whether these phonons are due to “folding” of phonon dispersion relations[4]. However, so far, study seems to be leading to the fact that the phonons observed are not due to “folding.” One hypothesis is that these optical phonons are caused by the defects at the interfaces of the alternating superlattice periods.

II. EXPERIMENTAL METHOD

The AlN/GaN superlattices in this work have been grown by molecular beam epitaxy on a thin (30-70nm) GaN buffer layer which was deposited on a sapphire substrate. Each superlattice is made of 300 periods. A period consist of n monolayers of AlN plus m monolayers

of GaN, where $0 < m, n \leq 8$. Different superlattices have been studied which vary is layer thickness and thickness ratio.

Room temperature infrared reflection spectroscopy measurements were taken at oblique incidence of 75° as shown in Fig. 1.

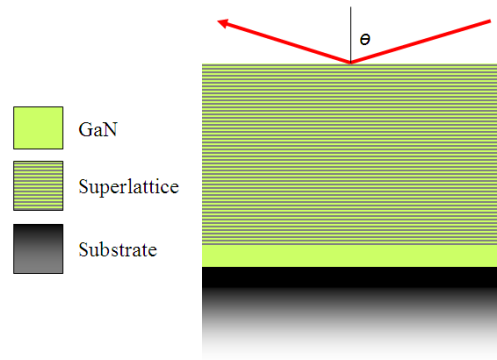


FIG. 1: Cross-sectional view of sample showing layers and the angle of incident.

III. THEORY

Calculating the dielectric function of the semiconductor material is important in relating phonon frequencies to the reflection spectrum. This is accomplished using the expression

$$\epsilon(\omega) = \epsilon_\infty + \sum_{j=1}^m \frac{4\pi F_j}{\omega_{Tj}^2 - \omega^2 - i\omega\gamma_{Tj}}, \quad (1)$$

where ϵ_∞ is the high-frequency dielectric constant and F_j , ω_{Tj} , and γ_{Tj} are the j th-mode oscillator strength, transverse optical (TO) phonon frequency, and damping respectively. Also, oscillator strength is a function of transverse and longitudinal optical (LO) phonon

frequencies[5]:

$$F_j = \frac{\epsilon_\infty}{4\pi} (\omega_{Lj}^2 - \omega_{Tj}^2) \prod_{k \neq j}^m \frac{\omega_{Lk}^2 - \omega_{Tj}^2}{\omega_{Tk}^2 - \omega_{Tj}^2}, \quad (2)$$

In general, the dielectric function can be separated into real and imaginary parts, $\epsilon(\omega) = \epsilon'(\omega) + i\epsilon''(\omega)$. The imaginary part of the dielectric function $\epsilon''(\omega)$ is the energy absorbed as a function of frequency and therefore directly affects the reflection spectrum of that material[6].

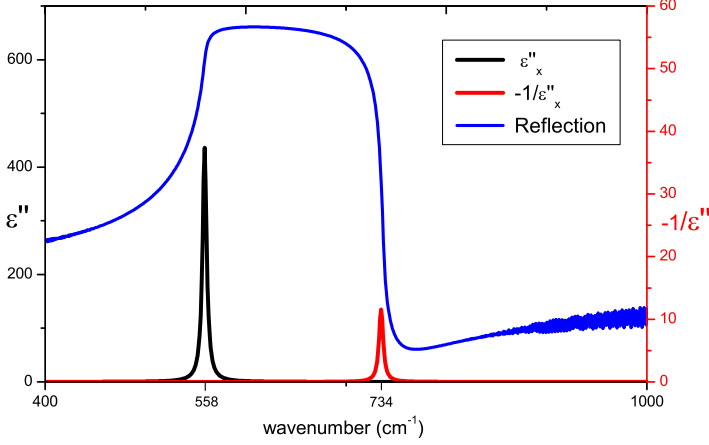


FIG. 2: Reflection spectrum of bulk GaN calculated with the plotted dielectric function $\epsilon''(\omega)$ and $-1/\epsilon''(\omega)$. The optical phonon frequencies of GaN are shown on the x-axis in wavenumber $\tilde{\nu} = \omega/c$. The reflection y-axis is not shown which ranges from 0 to 1.

Fig. 2 shows a simple example of how optical phonon frequencies affect the imaginary part of the dielectric function $\epsilon''(\omega)$. The transverse optical (TO) phonon is at 558_x cm^{-1} , and the longitudinal optical (LO) phonon in GaN is at 734_x cm^{-1} . These phonon frequencies are where the dielectric functions $\epsilon''(\omega)$ and $-1/\epsilon''(\omega)$ peak. Light with frequencies between the TO and LO phonons is reflected as shown in the GaN spectrum. The total unpolarized reflection \mathcal{R}_u is calculated from the s - and p -polarized components[7]:

$$\mathcal{R}_s(\omega) = \left| \frac{\cos \theta_i - [\epsilon_x(\omega) - (\sin^2 \theta_i)]^{\frac{1}{2}}}{\cos \theta_i + [\epsilon_x(\omega) - (\sin^2 \theta_i)]^{\frac{1}{2}}} \right|^2, \quad (3)$$

$$\mathcal{R}_p(\omega) = \left| \frac{\frac{1}{\epsilon_x^{\frac{1}{2}}(\omega)} \cos \theta_i - [1 - (\sin^2 \theta_i)/\epsilon_z(\omega)]^{\frac{1}{2}}}{\frac{1}{\epsilon_x^{\frac{1}{2}}(\omega)} \cos \theta_i + [1 - (\sin^2 \theta_i)/\epsilon_z(\omega)]^{\frac{1}{2}}} \right|^2, \quad (4)$$

$$\mathcal{R}_u(\omega) = \frac{1}{2} (\mathcal{R}_s(\omega) + \mathcal{R}_p(\omega)), \quad (5)$$

For bulk materials, the reflection spectrum is simply calculated with Eq. (3), (4), and (5). Notice in these equations that the reflection spectrum is strongly dependent on the dielectric function.

The reflection spectrum calculation becomes more complex in multilayered semiconductors due to the interfaces between the different materials that make up the sample. For simplicity, the superlattice (SL) is approximated to be one layer, reducing the sample to three layers: SL, GaN buffer, and sapphire substrate. Reflection due to each layer is calculated from Eq. (3), (4), and (5) as in bulk materials. Then the total multilayered reflection spectra can be computed from these results according to [7].

IV. MAPPING

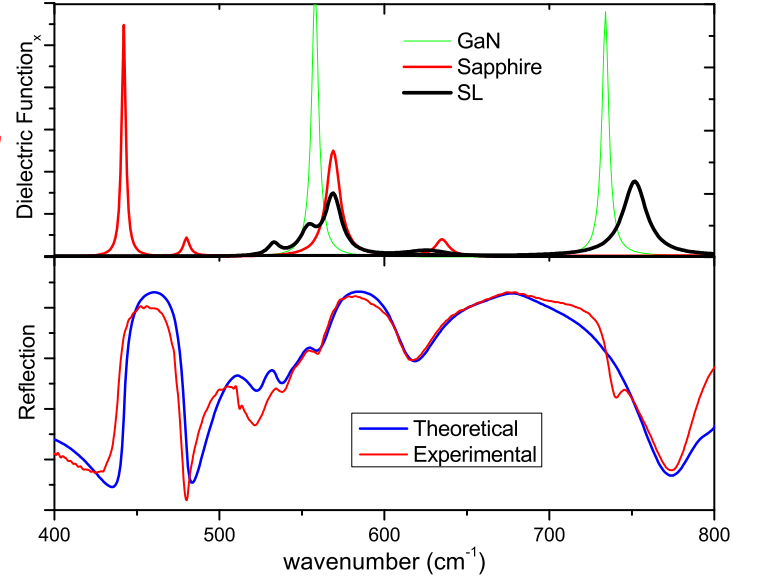


FIG. 3: Graph shows the reflection spectrum of AlN/GaN SL. Calculated and Experimental spectra are shown. Also the dielectric functions $\epsilon''_x(\omega)$ and $-1/\epsilon''_x(\omega)$ are plotted. Comparing this graph to Fig. 2, the similarities and additional complexities that arise in the layered structure can be seen.

The phonon frequencies of the SL which are input parameters to the theoretical calculations are adjusted until the calculations match infrared spectra experiments. The lower plot of Fig. 3 shows good mapping of experimental results. The local minima of experimental and theoretical spectra are the critical frequencies that are matched by tuning the SL phonon frequencies. Note that the strong reflectivity between $440\text{-}480 \text{ cm}^{-1}$ is due to the sapphire substrate. The substrate's transverse and longitudinal phonons at those frequencies seen in the upper graph form this reflected band. Therefore, the local minima less than 500 cm^{-1} are not matched with theoretical results. The low energies of the spectrum are not of interest in determining characteristic of phonons in the SL since phonon frequencies in the SL are greater than 500 cm^{-1} . The shift in the minima less than 500 cm^{-1} could be due to strain in the substrate[8]. The high reflectivity range from $550\text{-}740 \text{ cm}^{-1}$ is primarily from GaN (as shown in Fig. 2), but much of the additional structure

in the reflectivity arises from SL phonons, especially in the $500\text{-}600\text{cm}^{-1}$ range.

V. RESULTS

Six different SL samples were mapped to determine the new phonon modes that arise from the SL periods. Fig. 4 shows new phonons that are created in the superlattices. Bulk AlN has optical phonons at approximately 900 cm^{-1} and 660 cm^{-1} as shown on the right side of the graph while bulk GaN has optical phonons near 558 cm^{-1} and 734 cm^{-1} (plotted on left). The additional phonons in the center of the graph ($\omega_{Lx2}, \omega_{Tx2}, \omega_{Lx3}, \omega_{Tx3}$, etc.) are due to the periodic atomic SL structure.

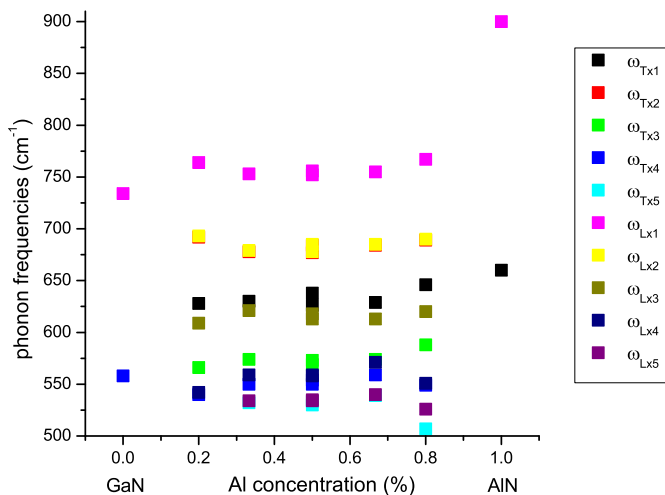


FIG. 4: Plot shows all the new phonon modes that arise in the AlN/GaN superlattices. Plotted on the edges are the phonon modes in bulk AlN and GaN. The samples between have additional frequencies that are due to new mode oscillations

It has been suggested that these additional phonons can be predicted and calculated by “folding” the bulk material’s dispersion curves[4]. In the superlattice the unit cell is now larger since the basis group is made up of m pairs of Al and N atoms and n GaN pairs. This increase in the hexagonal unit cell height cause a decrease in the Brillouin Zone (BZ). For example, in bulk material the k -vector at the BZ edge is $2\pi/d$, where $d \equiv c_0$, while in an $\text{AlN}_2/\text{GaN}_2$ SL the BZ edge k -vector is π/c_0 since the unit cell height is doubled, i.e. $d \equiv 2c_0$.

Fig. 5 illustrates this method for estimating the dispersion curve of $\text{AlN}_2/\text{GaN}_2$ (2x2) by folding the reduced wavevector BZ. The middle plot (1x1) shows one fold which is the estimate of a $\text{AlN}_1/\text{GaN}_1$ phonon dispersion curve. None of the samples studied were $\text{AlN}_1/\text{GaN}_1$ SL, therefore, $\text{AlN}_2/\text{GaN}_2$ is the simplest example. The phonons which were experimentally measured for this 2x2 SL are plotted at the zone center, Γ , since this is approximately where light would intersect the dispersion curve.

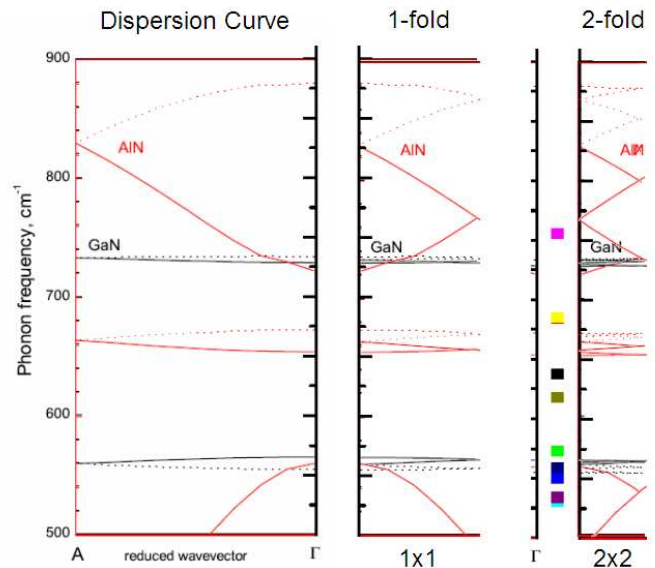


FIG. 5: Estimated dispersion relation of $\text{AlN}_2/\text{GaN}_2$ SL determined by “folded” dispersion curves of bulk AlN and GaN. The data points on the right are the TO and LO phonons determined to be present in $\text{AlN}_2/\text{GaN}_2$ obtained from Fig. 4

A cluster of data points match with the 2-fold dispersion curve near 560cm^{-1} where many phonons are predicted. However, there are also phonons that are detected that do not match up with this estimation: the phonon near 620cm^{-1} , for example. The dispersion relation folding is known to be useful in determining acoustic modes in SL; however, optical modes seem to be present more as confined modes[4].

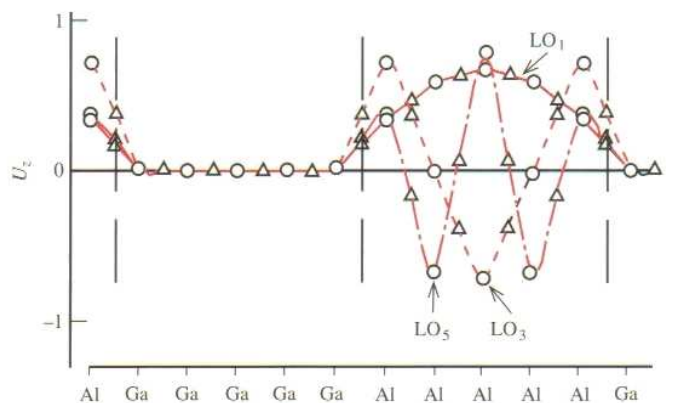


FIG. 6: Displacement pattern for confined LO modes in $\text{GaN}_5/\text{AlN}_5$ superlattice. The triangles represent the magnitude of the displacement of the N atoms while the circles represent that for Ga and Al[4].

The superlattices are made up of N, Al, and Ga atoms which masses are 14amu , 27amu , and 69.7amu respectively. Since the N atoms are the lightest they will vibrating the most, then Al. Ga atoms will be relatively stationary. The SL periods alternate between a layer

made of Al and N atoms followed by a layer with N and heavier Ga atoms. The dense GaN atomic layers confine phonon modes in the AlN layers which are made up of lighter atoms, similar to how electrons are confined in quantum wells. It is also possible for the GaN layers to confine phonons, however, this usually only occurs when the GaN layer is surrounded by thick AlN layers which act as barriers[4].

Theories and calculation have been made to predict these confined LO modes[9]. Results from [9] have been compared with experimental results in this work to determine if these confined mode calculation account for the SL optical phonons. Yet still, there are certain LO

modes that are not accounted for.

VI. CONCLUSION

In GaN/AlN superlattices new optical phonon modes are measured. Some theories have determined the existence of certain modes. However, the cause of the other phonon energy levels is still unknown. One possible hypothesis is that the new modes are due to impurities, dislocations, or strain within the superlattice[8]. Future work will be conducted to examine these possibilities.

-
- [1] M. Lundsrom, *Fundamentals of Carrier Transport* (Cambridge, 2000).
 - [2] C. Kumtornkittikul, I. Waki, N. Lia, M. Sugiyama, Y. Shimogaki, and Y. Nakano, TENCON 2004 (IEEE Region 10 Conference) **Nov. 2004**, 140 (2004).
 - [3] A. S. Barker and M. Ilegems, *Phys. Rev. B* **7**, 743 (1973).
 - [4] P. Y. Yu and M. Cardona, *Fundamentals of Semiconductors: Physics and Materials Properties* (Springer, 2001).
 - [5] C. T. Kirk, *Phys. Rev.* **38**, 1255 (1998).
 - [6] J. Merz, electromagnetic theory lecture notes.
 - [7] O. E. Piro, *Phys. Rev. B* **36**, 3427 (1987).
 - [8] A. M. Mintrairov (Fall 2006), communicated.
 - [9] A. M. Mintrairov, A. Vlasov, J. L. Merz, D. Korakakis, T. Moustakas, A. Osinsky, R. Gaska, and M. Smirnov, *Mat. Res. Soc. Symp. Proc.* pp. 427–432 (Spring 1999).